Available online at www.sciencedirect.com
ScienceDirect
Geochimica et Cosmochimica Acta 70 (2006) 4477–4490
Geochimica
www.elsevier.com/locate/gca

Reaction of $Mn^{III,IV}$ (hydr)oxides with oxalic acid, glyoxylic acid, phosphonoformic acid, and structurally-related organic compounds

Yun Wang *,[1], Alan T. Stone

Department of Geography and Environmental Engineering, G.W.C. Whiting School of Engineering, The Johns Hopkins University, Baltimore, MD 21218, USA

Received 24 October 2005; accepted in revised form 19 June 2006

Abstract

Phosphonoformic acid, oxalic acid, glyoxylic acid, and 10 additional organic compounds that are structurally related to them have been reacted with synthetic MnO_2 (birnessite), consisting of 22% Mn^{III} and 78% Mn^{IV}, and synthetic MnOOH (manganite), consisting solely of Mn^{III}. Significant concentrations of dissolved Mn^{III} were detected in reactions of phosphonoformic acid with MnOOH, indicating that ligand-assisted dissolution took place. Reaction of phosphonoformic acid with MnO_2, and reaction of all other organic reactants with either MnOOH or MnO_2, yielded only Mn^{II}, indicating that reductive dissolution was predominant. As far as reductive dissolution reactions are concerned, MnO_2 yields a range of reactivity that is nearly 20-times greater than that of MnOOH. Oxidation converts phosphonoformic acid into orthophosphate ion, glyoxylic acid into formic acid, pyruvic acid into acetic acid, and 2,3-butanedione into acetic acid. When differences in surface area loading are accounted for, oxalic acid, pyruvic acid, and 2,3-butanedione yield virtually the same dissolution rates for the two (hydr)oxides. At pH 5.0, glyoxylic acid reacts 14-times faster with MnO_2 than with MnOOH. MnO_2 reacts more slowly than MnOOH by a factor of 1/16th with oxamic acid, 1/20th with lactic acid, and 1/33rd with dimethyl oxalate. Adsorptive, complexant, and reductant properties of the 13 organic reactants are believed responsible for the observed reactivity differences.

1. Introduction

Organic compounds possess adsorptive, complexant, and reductant properties that determine pathways and rates of reactions with inorganic constituents (Stone et al., 1994; Stone, 1997). Here, we are interested in reactions with Mn (hydr)oxides. Soils and sediments often contain (hydr)oxides that are a mixture of Mn^{III} and Mn^{IV} (Kalhorn and Emerson, 1984; Guest et al., 2002), although pure Mn^{IV} phases also exist (Murray et al., 1984). Adsorptive properties are responsible for the formation of surface complexes that are the prerequisite of all reactions at (hydr)oxide surfaces (Stumm, 1992). Complexant properties can lead to the detachment of surface-bound Mn^{III} and the formation of Mn^{III}-organic complexes in solution, a process termed ligand-assisted dissolution (Kostka et al., 1995; Klewicki and Morgan, 1999). Reductant properties make possible the conversion of Mn^{IV} and Mn^{III} to much more soluble Mn^{II}, a process termed reductive dissolution (Stone, 1987b).

What do we know about the reaction of aliphatic organic compounds with Mn (hydr)oxides? Stone (1987a), employing a phase consisting of 18% Mn^{III} and 82% Mn^{IV}, observed that decreasing the pH from 6.0 to 5.0 yielded a 23-fold increase in the rate of dissolved Mn production by oxalic acid, and a threefold increase in the rate of dissolved Mn production by pyruvic acid. Correcting for differences in surface area loading, Xyla et al. (1992)

* Corresponding author.
E-mail address: yunwang@gps.caltech.edu (Y. Wang).
[1] Present address: Division of Geological and Planetary Sciences, and Howard Hughes Medical Institute, Mail Code 100-23, California Institute of Technology, Pasadena, CA 91125, USA.

0016-7037/$ - see front matter © 2006 Published by Elsevier Inc.
doi:10.1016/j.gca.2006.06.1548

observed that rates of dissolved Mn production following oxalic acid addition at pH 4.0 decreased in the order MnOOH (manganite) > MnO_2(birnessite) > MnO_2(pyrolusite). Godtfredsen and Stone (1994) pre-equilibrated a (hydr)oxide consisting of 14% Mn^{III} and 86% Mn^{IV} with Cu^{II}. Sorption/desorption of Cu^{II} provided information about competitive adsorption, surface site loss, and complex formation in solution during dissolution by pyruvic acid, oxalic acid, and citric acid. Klewicki and Morgan (1999) used UV–visible spectrophotometry to prove that dissolved Mn^{II} and Mn^{III} are both generated when citric acid is reacted with a mixed (hydr)oxide with an average Mn oxidation state close to +3.0. In addition, Luther et al. (1999) employed UV–visible spectrophotometry to examine the reaction of colloidal MnO_2 with oxalic acid.

More recently, we investigated the reaction of citric acid with a MnO_2(birnessite) phase consisting of 22% Mn^{III} and 78% Mn^{IV} (Wang and Stone, 2006). Although most of the dissolved Mn product is in the +II oxidation state, 1–5 μM concentrations of the +III oxidation state are also detectable using capillary electrophoresis (Wang and Stone, 2006). Monitoring citric acid loss and the production of the oxidation products ketoglutaric acid and acetoacetic acid by capillary electrophoresis helped establish that the strong autocatalytic nature of this reaction arises from the oxidation of Mn^{II}-citrate complexes by surface-bound $Mn^{III,IV}$ (Wang and Stone, 2006).

Our objectives in the present work are threefold: (i) to provide an understanding of the connection between aliphatic organic compound structure and reactivity, by investigating a wider range of organic reactants than attempted in past studies; (ii) to distinguish dissolved Mn^{II} production from dissolved Mn^{III} production using capillary electrophoresis; and (iii) when possible, to identify organic oxidation products using capillary electrophoresis.

The 13 aliphatic organic compounds selected for study (Table 1) all possess a carboxylic acid (RC(O)OH), a carboxylic acid methyl ester ($RC(O)OCH_3$), or a carbonyl group. Six have two such groups in an α-position relative to one another. Four have an alcohol group, one has a phosphonic acid ($RP(O)(OH)_2$) group, and one has a phosphonic acid ethyl ester group ($RP(O)(OH)(OCH_2CH_3)$ in the α-position. Two have amine groups ($-NH_2$) bonded to the carbonyl carbon. Inductive and resonance interactions among the functional groups just described affect ease of oxidation. Carboxylate and phosphonate groups are effective at coordinating metal ions in solution, facilitating adsorption (Kummert and Stumm, 1980; Filius et al., 1997; Nowack and Stone, 1999), and in some cases, assisting dissolution (Furrer and Stumm, 1986; Klewicki and Morgan, 1999).

Several of these small aliphatic organic compounds are of considerable biogeochemical importance. Oxalic acid is exuded by the roots of all vascular plants (Marschner, 1995); its concentration near growing root tips may reach 1.0 mM (Fox and Comerford, 1990). Release of pyruvic acid, lactic acid, glyoxylic acid, glycolic acid, and 2-hydroxyisobutyric acid by plant roots, bacteria, and fungi yields measurable concentrations in soil interstitial waters (Fox and Comerford, 1990; Afif et al., 1995; Madigan et al., 2002). A number of the compounds also have anthropogenic sources. Oxalic acid is used as an industrial cleansing agent (Sellers, 1983). Phosphonoformic acid is an pyrophosphate mimic that serves as an antiviral agent (Lindqvist and Nordstrom, 2001). Fosamine is an herbicide (Ware, 2000) and oxamic acid is a photolysis product of the herbicide picloram (Woodburn et al., 1989).

2. Materials and methods

All solutions were prepared from reagent grade chemicals without further purification, and distilled, deionized water (DDW) with a resistivity of 18 MΩ cm (Millipore Corp., Milford, MA). Filter holders (Whatman Scientific, Maidstone, England) were soaked in 1 N ascorbic acid (Aldrich, Milwaukee, WI) and rinsed with distilled water and DDW. All bottles and glassware for MnO_2 (birnessite) and MnOOH (manganite) suspensions were first soaked in 1 N ascorbic acid and rinsed with distilled water; and were next put in a 4 N nitric acid (J.T. Baker, Phillipsburg, NJ) bath overnight and rinsed with distilled water and DDW water prior to use.

2.1. Chemicals

Formic acid, glyoxylic acid, glycolic acid, 2,3-butanedione, 3-hydroxy-2-butanone, dimethyl oxalate, DL-lactic acid, 2-hydroxyisobutyric acid, urea, phthalic acid, benzoic acid, 2-sulfobenzoic acid, ascorbic acid, H_2O_2 (hydrogen peroxide), KCl, $ZnCl_2$, $MnSO_4 \cdot H_2O$, and $NiCl_2 \cdot 6H_2O$ were purchased from Aldrich. Oxamic acid, pyruvic acid, phosphonoformic acid, and disodium pyrophosphate were purchased from Fluka (Buchs, Switzerland). Potassium oxalate was purchased from Sigma (St. Louis, MO). Fosamine ammonium was purchased from Chem Service (West Chester, PA). HCl, NaOH, NaCl, NaH_2PO_4, and Na_2HPO_4 were purchased from J.T. Baker. $CaCl_2 \cdot 2H_2O$ was purchased from Fisher Chemical (Pittsburgh, PA). Sodium butyrate (Aldrich), 2-morpholinoethansulfonic acid monohydrate (MES; Fluka), 3-[*N*-morpholino]propanesulfonic acid (MOPS; Sigma), and tris(hydroxymethyl) aminomethane (Tris; Aldrich) were used as pH buffers.

2.2. Preparation of MnO_2 and MnOOH

MnO_2 herein refers to particles synthesized according to the method of Luo et al. (2000); details of the synthesis and characterization are provided elsewhere (Wang and Stone, 2006). Diffraction lines obtained by X-ray diffraction are consistent with a distorted birnessite structure. A B.E.T. surface area of 174 m^2/g was determined using a freeze-dried sample. The average Mn oxidation state was found to be +3.78 based upon iodometric titration. If we assume that the Mn^{II} content is negligible, then the (hydr)oxide

Table 1
Properties and initial rates for reaction of MnO_2 and MnOOH at pH 5.0 with 13 organic reactants

Chemical name	Structure	pK_as[a]	$R_0(MnO_2)$ ($\mu M h^{-1}$)	R_0(MnOOH) ($\mu M h^{-1}$)	$R_A(MnO_2)$ ($\mu mol\ m^{-2}\ h^{-1}$)	R_A(MnOOH) ($\mu mol\ m^{-2}\ h^{-1}$)	$\frac{R_A(MnO_2)}{R_A(MnOOH)}$
Glyoxylic acid	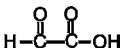	3.46	$>3.0\times10^{3}$	3.2×10^{1}	8.9×10^{2}	6.4×10^{1}	1.4×10^{1}
Phosphonoformic acid[b]	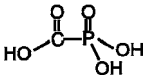	1.92 4.04 8.23	$\sim1.4\times10^{3}$	7.7×10^{1}	4.1×10^{2}	1.5×10^{2}	2.7×10^{0}
Oxalic acid	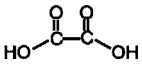	1.25 4.27	4.6×10^{2}	7.0×10^{1}	1.4×10^{2}	1.4×10^{2}	9.8×10^{-1}
Pyruvic acid	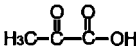	2.48	6.8×10^{1}	1.2×10^{1}	2.0×10^{1}	2.4×10^{1}	8.4×10^{-1}
2,3-Butanedione	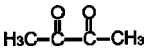		3.0×10^{1}	3.6×10^{0}	8.9×10^{0}	7.2×10^{0}	1.2×10^{0}
3-Hydroxy-2-butanone	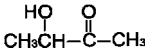		—	1.6×10^{0}	—	3.2×10^{0}	—
Glycolic acid	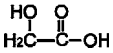	3.83	1.4×10^{1}	4.7×10^{0}	4.1×10^{0}	9.4×10^{0}	4.4×10^{-1}
Oxamic acid	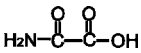	2.5[c]	4.8×10^{0}	1.1×10^{1}	1.4×10^{0}	2.2×10^{1}	6.5×10^{-2}
Dimethyl oxalate	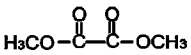	11.8[c]	2.7×10^{0}	1.3×10^{1}	8.0×10^{-1}	2.6×10^{1}	3.1×10^{-2}
DL-Lactic acid	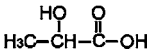	3.86	1.6×10^{0}	4.7×10^{0}	4.7×10^{-1}	9.4×10^{0}	5.0×10^{-2}
2-Hydroxyisobutyric acid	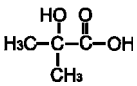	4.03	2.7×10^{-1}	1.3×10^{-1}	8.0×10^{-2}	2.6×10^{-1}	3.1×10^{-1}
Fosamine	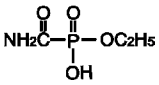	1–2[d]	7.0×10^{-2}	$<8.0\times10^{-2}$	2.1×10^{-3}	$<1.6\times10^{-1}$	$>1.3\times10^{-2}$
Urea	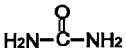	0.1	$<1.0\times10^{-2}$	$<8.0\times10^{-2}$	$<3.0\times10^{-3}$	$<1.6\times10^{-1}$	—

All experiments employed 200 μM (hydr)oxide and 5.0 mM organic reactant. Descriptions of how R_0 and R_A are calculated are found in the text.
[a] Unless otherwise noted, pK_a values are for 25 °C and infinite dilution conditions (ionic strength = 0), and were obtained from the CRITICAL database (Martell et al., 2004).
[b] The reaction between MnOOH and phosphonoformic acid is the only case where Mn^{III}(aq) was detectable. In this case, Mn^{II}(aq) is calculated as the difference between Mn_T(aq) and Mn^{III}(aq).
[c] From Leitner et al. (2002), the pK_a value of 2.5 is from the deprotonation of –COOH group; the pK_a value of 11.8 is from the deprotonation of $–NH_2$ group.
[d] Based upon known pK_as for other phosphonate monoesters (Kiss and Lazar, 2000), the pK_a is expected to be within this range.

consists of a mixture of 22% Mn^{III} and 78% Mn^{IV}. The freeze-dried particles weighed 97.1 g/mol of manganese.

MnOOH herein refers to particles synthesized according to the method of Giovanoli and Leuenberger (1969). Three thousand millilitres of 6.0×10^{-2} M $MnSO_4$ solution was stirred vigorously and heated to 60 °C, followed by quick addition of 62 mL of 8.82 M H_2O_2 solution and subsequent slow addition of 900 mL of 0.20 M NH_4OH solution. All three solutions were sparged with Ar (BOC gases, Baltimore, MD) before mixing. The resulting brown suspension was quickly heated to 95 °C; heating, stirring, and Ar sparging were maintained for 6 h. After overnight cooling, a washing procedure using centrifugation to collect the particles and sonication to resuspend the particles in fresh DDW was repeated 10-times. The pH of the washed suspension was approximately 7.0. After washing, the specific conductivity of the supernatant solution was less than that of a 1×10^{-4} M KCl solution. Dissolved manganese in the supernatant solution was less than the AAS detection limit (1.0 μM). The washed suspension aliquots were stored in a flash-frozen state.

Using X-ray diffraction, the following *d*-spacings, all consistent with the mineral manganite (Bricker, 1965), were obtained: 3.41, 2.65, 2.41, 2.28, 2.20, 1.78, and 1.67 Å. Transmission electron microscopy revealed needle-shaped

crystals of uniform size. Freeze-dried MnOOH yielded a B.E.T. surface area of 27.3 m^2/g. The freeze-dried particles weighed 91.5 g/mol of manganese.

2.3. Experimental setup

2.3.1. Dissolution experiments

All batch experiments were conducted in 100 mL polypropylene bottles in a constant temperature circulating bath at 25 ± 0.2 °C and stirred with Teflon-coated stir bars. To maintain constant pH, 10 mM butyrate ($4.0 < pH < 5.5$), MES ($5.5 < pH < 6.6$), or MOPS ($6.6 < pH < 7.5$) buffers were employed. pH stability was verified by periodic measurement (Fisher Accumet 825MP meter with Orion Combination semi-micro probe; NIST-traceable standards). pH buffer concentrations were high enough to serve an additional purpose: maintenance of constant ionic strength conditions. No additional electrolyte was added.

Solutions containing organic compound and pH buffer (plus additional constituents, as appropriate) were sparged with Ar for 1 h prior to MnO_2 or MnOOH addition. Sparging was continued during the duration of the experiments. 4mL reaction suspension aliquots were collected at periodic intervals. Reactions were quenched by immediately filtering through 0.1 μm pore diameter track-etched polycarbonate filter membranes (Whatman). Total dissolved manganese in the filtered solutions was analyzed using flame atomic absorption spectrophotometry (AAS: Analyst 100, Perkin-Elmer, Norwalk, CT). Mn AAS standard was purchased from Aldrich. Additional species in the filtered solutions were analyzed using capillary electrophoresis (see later section). Inorganic carbonate was not monitored due to possible losses arising from sparging.

2.3.2. Adsorption experiments

All experiments began by adding MnO_2 stock suspension, solution of the test compound (acetic acid or methylphosphonic acid), NaCl and DDW into 15 mL polypropylene bottles. Prior to use, DDW was sparged with Ar overnight to eliminate inorganic carbonate. Sparging was continued during the duration of the experiments. The pH was set by the addition of HCl or NaOH. NaCl stock solution was added to ensure that the ionic strength was at least 1.0 mM. Accounting for other system constituents yields a calculated ionic strength in the low mM range. A circulating constant temperature bath maintained the temperature at 25.0 ± 0.2 °C. Stirring was performed using teflon-coated stir bars. Suspensions were equilibrated for 4 h prior to filtration through 0.1 μm pore diameter track-etched polycarbonate filter membranes (Whatman). The concentrations of the test compound in the filtered solutions were analyzed using capillary electrophoresis (see later section). The extent of adsorption was obtained by subtracting the concentration measured in supernatant solution from the total added concentration. To confirm that degradation of acetic acid or methylphosphonic acid was not taking place, experiments were conducted where each was recovered from the MnO_2 surface by raising the pH to 12, which caused both compounds to desorb.

2.4. Capillary electrophoresis

A capillary electrophoresis unit from Beckman Coulter (P/ACE MDQ, Fullerton, CA) with diode-array UV–visible detector was used for all determinations. Bare fused silica capillaries (Polymicro Technologies, Phoenix, AZ) with 75 μm ID × 60 cm total length were used for all separations. The effective length, defined as the length from the inlet to the detector, was 52 cm. Capillary and sample board temperature was thermostatted to 10 °C during operation. Between separations, the capillary was sequentially rinsed by flushing with DDW for 0.5 min, with 0.1 N NaOH for 1 min, with DDW again for 1 min, and with capillary electrolyte for 2 min. Sample injection employed 0.5 psi of positive pressure for 15 s.

Mn^{III}(aq) (total dissolved Mn^{III}) was measured using a direct UV photometric method described in detail elsewhere (Wang and Stone, 2006). The CE electrolyte consisted of 20 mM pyrophosphate buffer (pH 7.5) and 0.4 mM tetradecyltrimethylammonium bromide (TTAB: Aldrich) electroosmotic flow modifier. Anion mode with a constant applied voltage of −22 kV was used. The pyrophosphate concentration is high enough and Mn^{III} is sufficiently labile that all Mn^{III}-containing species in the sample are converted into Mn^{III}-pyrophosphate complexes upon contact with the CE electrolyte solution (Wang and Stone, 2006). A sharp, symmetrical peak, easily discernable at a detection wavelength of 235 nm, provided the means of measuring Mn^{III}(aq) (total dissolved Mn^{III}). The detection limit for Mn^{III}(aq) was about 1.5 μM at this wavelength. This method allows for the simultaneous determination of Mn^{III}(aq) and any organic chromophores present in the sample.

With oxalic acid, direct UV detection at 190 nm worked well. For all other organic analytes, indirect photometric detection was employed. Ionized chromophores 2-sulfobenzoate, phthalate, or benzoate were place in the CE electrolyte, and a detection wavelength of 200 nm was employed (electromigrating analyte molecules displace chromophoric ions in the CE electrolyte, yielding negative peaks which can be quantified.). Table S1, Electronic annex matches each analyte with the corresponding CE technique.

2.5. Data analysis

Initial rates of Mn^{II}(aq) production (R_i, in units of μM/h) were obtained from the slopes of concentration versus time plots. Unless otherwise stated, the slope corresponds to the least-squares fit of four or more data points collected during the first 20% of dissolution. r^2 values were typically greater than 0.95.

At pH 5.0, both MnO_2 and MnOOH gradually released dissolved Mn^{II}, even in the absence of organic reactant. Background dissolution rates measured in 10 mM butyrate

buffer (pH 5.0) were 1.0×10^{-2} μM/h for 200 μM MnO_2 and 8.0×10^{-2} μM/h for 200 μM MnOOH. When organic reactants are present, we will assume that the gradual release of Mn^{II} just described proceeds in parallel. Dissolution rates arising from reaction with the organic reactant, which we will call R_0, are calculated by subtracting the background rates from R_i.

The two manganese (hydr)oxides employed in this work possess different surface areas. In order to make reactivity comparisons, differences in surface area loading need to be accounted for. For each (hydr)oxide, the area loading (in m^2 surface/L) is found by multiplying the B.E.T. surface area (in m^2/g) times the formula weight (g/mol of Mn) times the suspension concentration employed (in moles Mn/L). Dividing R_0 by the area loading yields R_A ($\mu mol \cdot m^{-2} h^{-1}$), the area-corrected rate.

Equilibrium calculations were performed using the software package *MINEQL* + (Schecher and McAvoy, 2003) and the equilibrium constants listed in Table S2, Electronic annex. Activity corrections were performed using the Davies equation (Stumm and Morgan, 1996, p. 103).

3. Results and discussion

3.1. Adsorption experiments

Methylphosphonic acid and acetic acid are selected for adsorption studies for two reasons: (i) they are archetypes for more complex phosphonic- and carboxylic-containing organics and (ii) they are not susceptible to degradation during the timescale for adsorption studies. To confirm that degradation was not taking place, desorption experiments were conducted by raising the pH to 12 after 4 h of reaction. Both compounds were fully recovered from the MnO_2 surface.

In suspensions containing 50 μM methylphosphonic acid (or acetic acid) and 51.5 mM MnO_2, adsorption of both compounds increases with decreasing pH (Fig. 1).

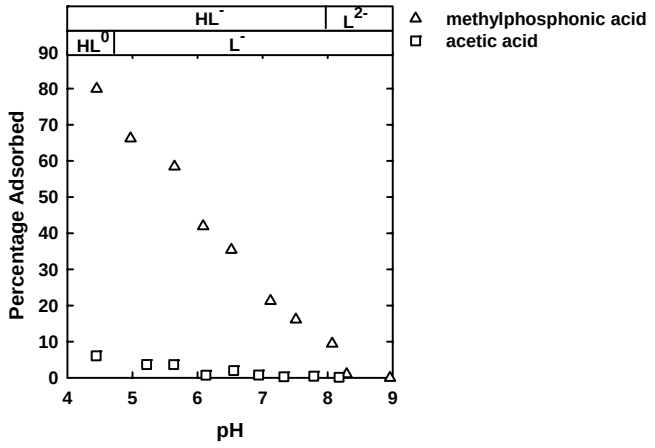

Fig. 1. Adsorption of 50 μM methylphosphonic acid and acetic acid onto 51 mM MnO_2 as a function of pH. All suspensions contained 1.0 mM NaCl. pH was set using HCl/NaOH addition. Top, two bars denote predominant protonation level domains (at an ionic strength of 1.0 mM).

For methylphosphonic acid, adsorption increases from negligible levels at pH values above 8.2 to nearly 80% at pH 4.4. For acetic acid, adsorption increases from negligible levels at pH values above 6.0 to nearly 6% at pH 4.4. At pH 5.0, the extent of adsorption is 14-times higher for methylphosphonic acid than for acetic acid. In order to discern adsorption, a MnO_2 loading 255-times what was used in dissolution experiments is required.

3.2. Oxidation products

Owing to the high resolution power of capillary electrophoresis, any peak that grows upon addition of authentic standard is considered positively identified. Experiments with both MnO_2 and MnOOH yielded conversion of phosphonoformic acid into orthophosphate ion, glyoxylic acid into formic acid, pyruvic acid into acetic acid, and 2,3-butanedione into acetic acid. For the other organic reactants listed in Table 1, reaction was either too slow for products to be discerned with the timescale of our experiments, or the CE methods listed in Table S1, Electronic annex did not yield new peaks. Inorganic carbonate, for example, which is believed to be an oxidation product for many of the compounds listed in Table 1, is not discernible by CE.

Balanced reactions for the conversion of organic reactants into oxidation products are presented in Fig. 2. In addition to our own observations, product structures reflect earlier work with dissolved Mn^{III} oxidants (e.g., Drummond and Waters, 1955; Levesley and Waters,

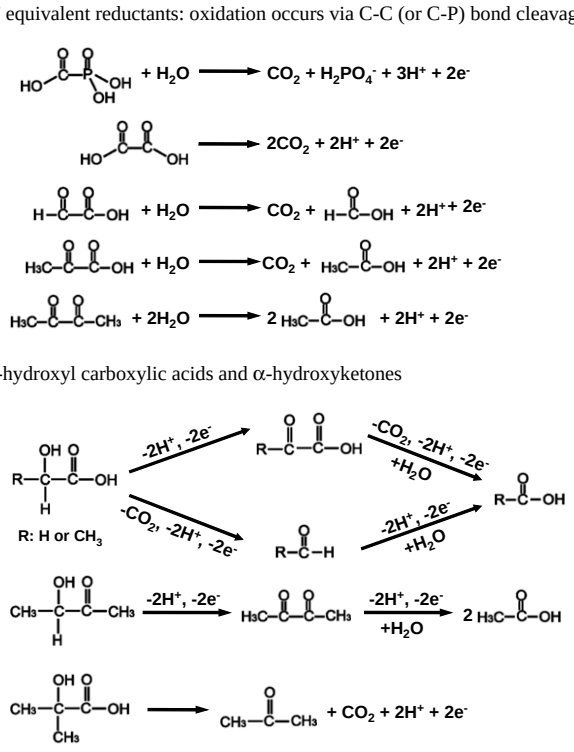

Fig. 2. Postulated schemes for organic reactant oxidation by MnO_2 and MnOOH. (a) $2e^-$ equivalent reductants: oxidation occurs via C–C (or C–P) bond cleavage. (b) α-Hydroxyl carboxylic acids and α-hydroxyketones.

1955; Kemp and Waters, 1964), with MnO_2 (birnessite) (Jauregui and Reisenauer, 1982) and with a variety of other transition metal oxidants, including chromate ion (Hasan and Rocek, 1975; Krumpolc and Rocek, 1977; Haight et al., 1985; Krumpolc and Rocek, 1985) and ferric ion (Thomas et al., 1960). Resonance interactions between alcohol, carbonyl, carboxylic acid, and phosphonic acid groups in an α-position relative to one another are undoubtedly important. With 3-hydroxy-2-butanone, glycolic acid, and lactic acid, abstraction of a hydrogen atom bonded to the carbon in the α-position relative to a carbonyl or carboxylic acid group is possible, where the radical generated (shown in brackets) is resonance-stabilized:

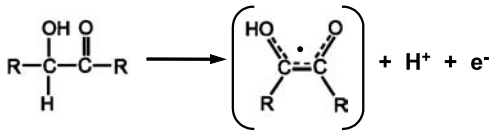

Decarboxylation is a common feature, e.g., with phosphonoformic acid, oxalic acid, glyoxylic acid, pyruvic acid, and α-hydroxyisobutyric acid Decarboxylation of α-hydroxyisobutyric acid during reaction with chromate ion has been observed (Krumpolc and Rocek, 1977; Krumpolc and Rocek, 1985).

3.3. Time course plots

Significant concentrations of dissolved Mn^{III} were detected when phosphonoformic acid was reacted with MnOOH (discussed more extensively later), but not with any other combination of organic reactant and manganese (hydr)oxide. Here, we are concerned solely with Mn^{II} production as a function of time. For reactions of phosphonoformic acid with MnOOH, we obtain $Mn^{II}(aq)$ by subtracting $Mn^{III}(aq)$ from $Mn_T(aq)$.

Fig. 3 shows $Mn^{II}(aq)$ as a function of time for reaction of 5.0 mM organic reactants with 200 μM MnO_2 at pH 5.0. Analogous time course plots for reactions with 200 μM MnOOH are shown in Fig. 4. Criteria for determining $dMn^{II}(aq)/dt$ were described in Section 2. Values of R_0 and R_A (rates corrected for differences in surface loading) are listed in Table 1. Our attention is focused primarily on initial rates. It is interesting to note, however, that rates as a function of reaction progress differ from one organic reactant to another. Glycolic acid reaction with MnO_2 yields nearly a zeroth-order plot of $Mn^{II}(aq)$ as a function of time, for example, while oxamic acid yields a lowering of rate as the reaction progresses.

Fig. 5 shows the loss of organic reactant, the formation of $Mn^{II}(aq)$, and the formation of organic oxidation product as a function of time for reaction of 200 μM organic reactants with 200 μM MnO_2 at pH 5.0. With phosphonoformic acid and glyoxylic acid, the sum [organic reactant] + [organic oxidation product] remains constant as the reaction progresses, indicating that mass balance is obeyed. Mass balance cannot be checked with oxalic acid reactions, since the sole oxidation product (inorganic carbonate) cannot be monitored.

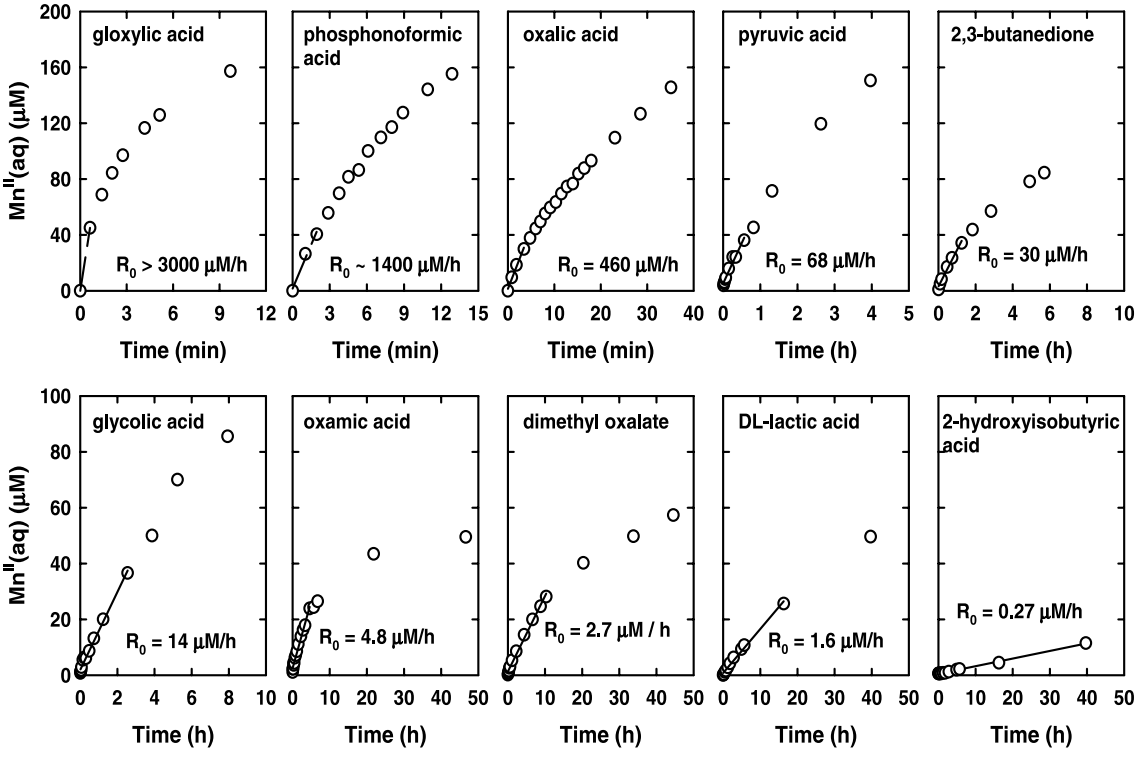

Fig. 3. Plots of $Mn^{II}(aq)$ production as a function of time for 200 μM MnO_2 reduction by 5.0 mM organics at pH 5.0 (10 mM butyrate-buffer).

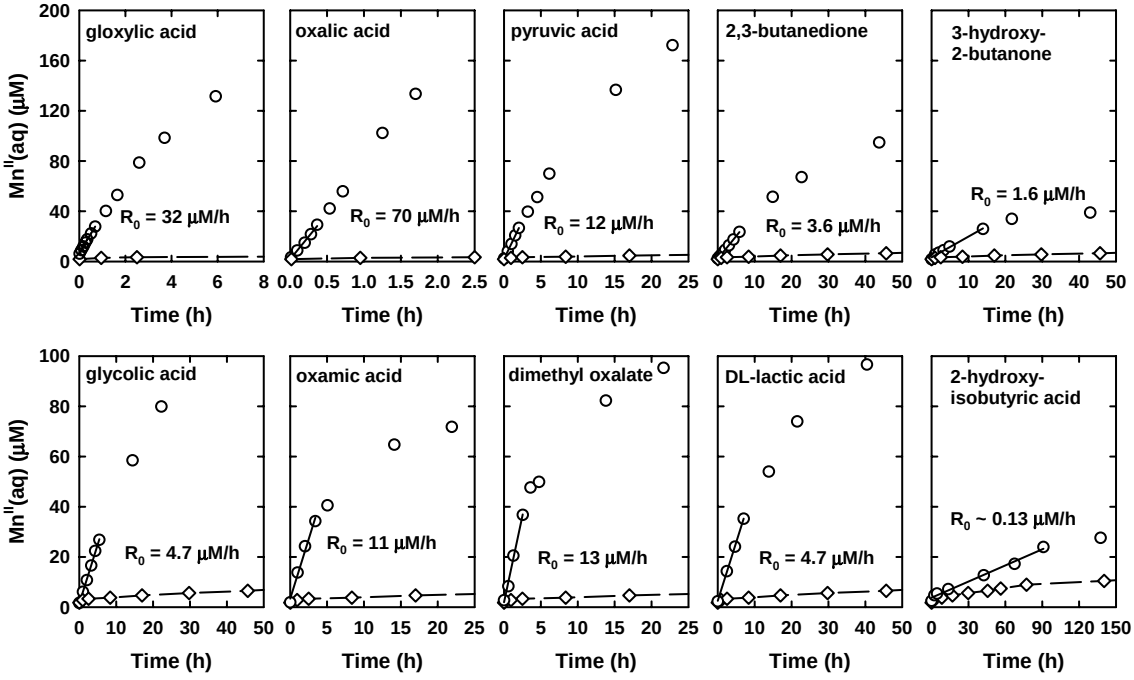

Fig. 4. Plots of Mn^{II}(aq) production as a function of time for 200 μM MnOOH reduction by 5.0 mM organics at pH 5.0 (10 mM butyrate-buffer). The symbol ◇ corresponds to Mn^{II}(aq) released in the absence of organic reactant.

3.4. MnO_2 reaction with glyoxylic acid, oxalic acid, and phosphonoformic acid

In every experiment involving these three reactants with MnO_2, Mn^{III}(aq) was below detectable levels. Total dissolved manganese (Mn_T(aq)) measured by AAS is therefore equivalent to total dissolved Mn^{II}. As shown in Fig. 6, a detailed investigation was conducted on the effects of pH on the reaction of 200 μM MnO_2 with 200 μM organic reactant. Regardless of pH, the order of reactivity observed is glyoxylic acid > phosphonoformic acid > oxalic acid. Orders with respect to [H^+] have been calculated as slopes between successive pairs of points on the logR_0 versus pH plot (Fig. 6). Near pH 7, both oxalic acid and phosphonoformic acid yield slopes considerably greater than 1.0, while glyoxylic acid yields a slope that is very near 1.0. Slopes diminish substantially as the pH is decreased. For all three compounds, slopes are nearly half-order with respect to [H^+] at the lowest pH values explored.

Repeating these experiments with a 25-fold increase in organic reactant concentration allows us to explore possible saturation behavior (Table 2). Phosphonoformic acid at pH 7.0 yields a rate increase that is nearly equal to the concentration increase. At pH 5.0 and 6.0, on the other hand, the rate increase is less than one-third the concentration increase, indicating saturation behavior. With glyoxylic acid and oxalic acid, only pH 5.0 data is available. A significant, although less pronounced saturation effect is observed.

Glyoxylic acid oxidation yields the readily quantified product formic acid. Comparing the yield of this product with that of Mn^{II} provides information regarding the surface reaction. Since manganese within the phase we employed exhibits an average oxidation state equal to +3.78, we will use $Mn(OH)_{3.78}$(s) to define reaction stoichiometry, i.e.:

$$\underset{\text{glyoxylate ion}}{HC(O)C(O)O^-} + 1.12Mn(OH)_{3.78}(s) + 2.22H^+ = \underset{\text{formate ion}}{HC(O)O^-} + CO_2 + 1.12Mn^{2+} + 3.23H_2O \quad (1)$$

The ratio of total moles of Mn^{II} produced, to total moles of formic acid produced, which we will call n, should be equal to 1.12. We can only measure dissolved Mn^{II} and formic acid, and hence we define an apparent yield, n′:

$$n' = \frac{[Mn^{II}(aq)]}{[\text{Formic acid(aq)}]} \quad (2)$$

Fig. 7 presents results from experiments employing 200 μM glyoxylic acid and 200 μM MnO_2 at four pH values. At all four pH values, final values of n' are in the range 1.2–1.3, somewhat higher than expected. At pH 5.0 and 5.5, early values of n' (less than 30 μM glyoxylic acid lost) are within 75% of final values. At pH 6.0 and 7.0, in contrast, early values of n' are only 46% of final values. It should be noted that the uncertainty associated with early values of n' is larger than with subsequent n' values, since quantities in both the numerator and denominator of Eq. 2 are close to analytical detection limits. Like glyoxylic acid, citric acid is a two-equivalent reductant. Values of n' from our previous work (Wang and Stone, 2006) are included in Fig. 7 for comparison.

In all four experiments, the sum [glyoxylic acid] + [formic acid] is constant, indicating that formic acid adsorp-

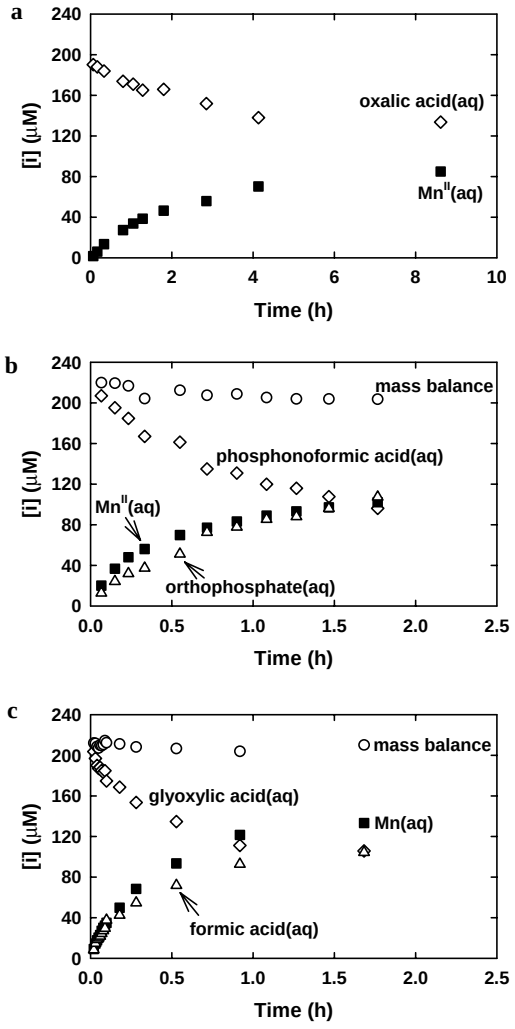

Fig. 5. Time course plots for reaction of 200 μM (a) oxalic acid, (b) phosphonoformic acid, and (c) glyoxylic acid with 200 μM MnO_2, in 10 mM butyrate buffer (pH 5.0). The mass balance refers to: (b) the sum [phosphonoformic acid (aq)] + [orthophosphate (aq)], (c) the sum [glyoxylic acid (aq)] + [formic acid (aq)].

tion and loss via oxidation are negligible. Low early values of n' may arise from either (i) reduction of Mn^{IV} in preference to Mn^{III}, or (ii) Mn^{II} adsorption. The second explanation is more likely for several reasons. Based on our previous study, the fraction of Mn^{II} adsorbed onto MnO_2 should rise dramatically as the pH is increased, e.g., between our two lowest and our two highest pH values (Wang and Stone, 2006). The fraction of Mn^{II} adsorbed should be highest early in the reaction; surface sites are consumed by reductive dissolution, and the surface becomes saturated with growing amounts of Mn^{II} (Godtfredsen and Stone, 1994). Citric acid is a considerably stronger ligand for Mn^{II} than glyoxylic acid, and hence should be able to solubilize a greater fraction of Mn^{II}.

Final values of n' that are somewhat higher than expected may reflect reaction with Mn^{III} in preference to reaction with Mn^{IV}. Recall Eq. 1; n' equal to 1.3 is what we would expect for a phase consisting of 46% Mn^{III} and 54% Mn^{IV}. Our phase contained only 22% Mn^{III}.

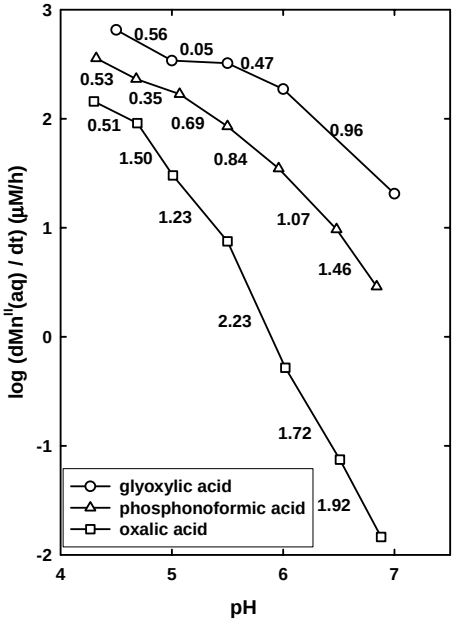

Fig. 6. Mn^{II}(aq) production as a function of pH for reaction of 200 μM MnO_2 with 200 μM glyoxylic acid, phosphonoformic acid, and oxalic acid. Suspensions contained either 10 mM butyrate (4.0 < pH 5.5), 10 mM MES (5.5 < pH < 6.6), or 10 mM MOPS (6.6 < pH < 7.5) buffer. For each successive pair of points, calculated reaction order with respect to $[H^+]$, obtained from the slope, are provided.

Table 2
Experiments performed using 200 μM and 5.0 mM organic reactant concentrations (and 200 μM MnO_2) allow possible saturation effects to be discerned

	R_0 (μMh^{-1})		$\frac{R_0(5.0\text{mM Organic})}{R_0(200\ \mu\text{M Organic})}$
	200 μM Organic	5.0 mM Organic	
Glyoxylic acid, pH 5.0	3.3×10^{2}	$>3.0\times10^{3}$	$>9.1\times10^{0}$
Oxalic acid, pH 5.0	3.0×10^{1}	4.6×10^{2}	1.5×10^{1}
Phosphonoformic acid			
pH 5.0	1.7×10^{2}	1.4×10^{3}	8.2×10^{0}
pH 6.0	3.5×10^{1}	2.8×10^{2}	7.9×10^{0}
pH 7.0	2.0×10^{0}	6.7×10^{1}	2.3×10^{1}

3.5. MnOOH reaction with glyoxylic acid, oxalic acid, and phosphonoformic acid

All experiments reported in this section employed 5.0 mM organic reactant and 200 μM MnOOH. With glyoxylic acid and oxalic acid, Mn^{III}(aq) was consistently below detection limits, similar to our findings with MnO_2. Phosphonoformic acid yielded significant dissolved Mn^{III} concentrations, and hence merits particular attention.

Time course plots for reaction of phosphonoformic acid with MnOOH at three different pH values are shown in Fig. 8. Overall rates of dissolution (reflected in Mn_T(aq)) increase dramatically as the pH is decreased, as indicated by the time interval shown by the three x-axes. Below each time course plot, a separate panel shows the fraction of dissolved Mn in the +III oxidation state.

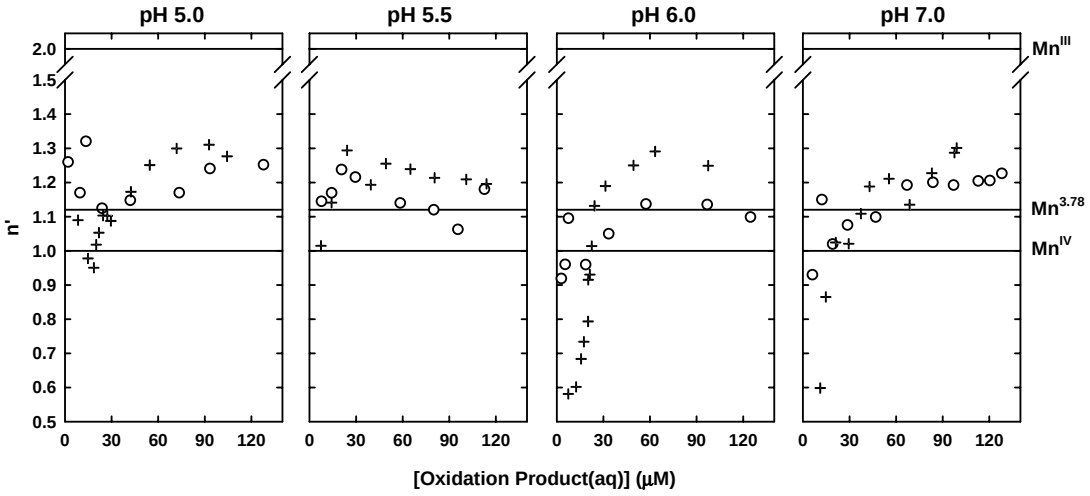

Fig. 7. Yield of Mn^{II} per mole of gloxylic acid (+) or citric acid (O) oxidized (see text). Data points (n') are calculated from experimentally determined dissolved concentrations. For glyoxylic acid, the pH 5.0 data correspond to the same experiment presented in Fig. 5c. For citric acid, the data come from Wang and Stone (2006). Horizontal lines correspond to expected values (n) for (hydr)oxides consisting solely of Mn^{III}, solely of Mn^{IV}, and a mixture with an average oxidation state of +3.78.

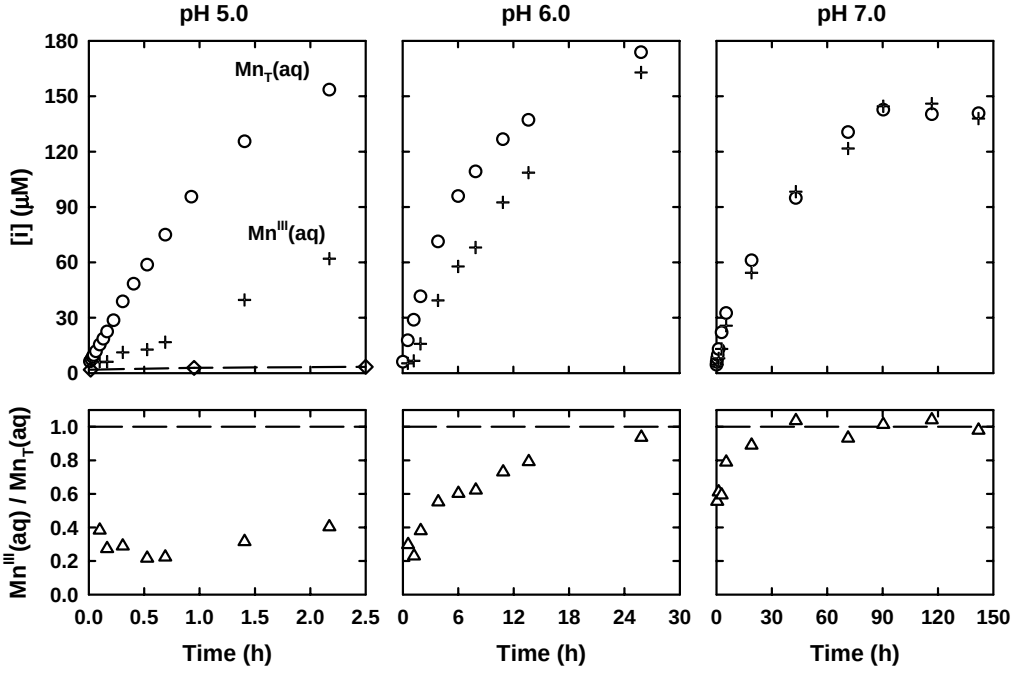

Fig. 8. Time course plots for the dissolution of 200 μM MnOOH by 5.0 mM phosphonoformic acid at three different pH values. The top three plots show Mn_T(aq) and Mn^{III}(aq), while the bottom three panels show the ratio Mn^{III}(aq)/Mn_T(aq). The pH was maintained by phosphonoformic acid self-buffering. In the top left plot, the symbol ◇ corresponds to Mn_T(aq) released in a phosphonoformic acid-free control experiment.

Caution is warranted with the earliest three data points; low values of Mn^{III}(aq) and Mn_T(aq) translate into relatively high uncertainty regarding the calculated fraction. It is quite apparent, however, that virtually all dissolved Mn is present in the +III oxidation state in the pH 7.0 experiment. At pH 6.0, the fraction in the +III oxidation state increases from somewhere below 50% to virtually all of the dissolved Mn as the reaction progresses. At pH 5.0, the fraction in the +III oxidation state lies between 20% and 40%.

We would like to compare rates of Mn^{II} production for the three organic reactants at pH 5.0 (this is the only pH where reactions with MnOOH for these three organic reactants were performed.). In the case of phosphonoformic acid, we assume that Mn^{II} production and Mn^{III} production are reactions in parallel. Mn^{II}(aq) is simply obtained by subtracting Mn^{III}(aq) from Mn_T(aq). R_0 (dMn^{II}(aq)/dt), as noted in Table 1, is slightly higher (~10%) for phosphonoformic acid than for oxalic acid. R_0 for oxalic acid is slightly more than twice the value calculated for glyoxylic acid.

3.6. Structurally-related organics

All 13 of the organic reactants listed in Table 1 were reacted at pH 5.0 with 200 μM MnO_2 and 200 μM MnOOH. A concentration of 5.0 mM was employed. Only urea failed to yield discernible dissolved Mn with both (hydr)oxides. Fosamine yielded the lowest rate among the other twelve compounds with MnO_2, and failed to yield a discernible rate with MnOOH. MnOOH yielded a 590-fold range in rates among the 11 remaining compounds. With MnO_2, the range of reactivity is far greater, more than 11,000-fold.

Surface area-corrected reaction rates (R_A values) provide the best comparison of the reactivity of MnOOH and MnO_2 (Table 1 and Fig. 9). R_A values for oxalic acid, pyruvic acid, and 2,3-butanedione are virtually the same for the two (hydr)oxides. Phosphonoformic acid reacts 2.65-times faster with MnO_2 than with MnOOH. 2-Hydroxyisobutyric acid reacts 3.3-times slower with MnO_2.

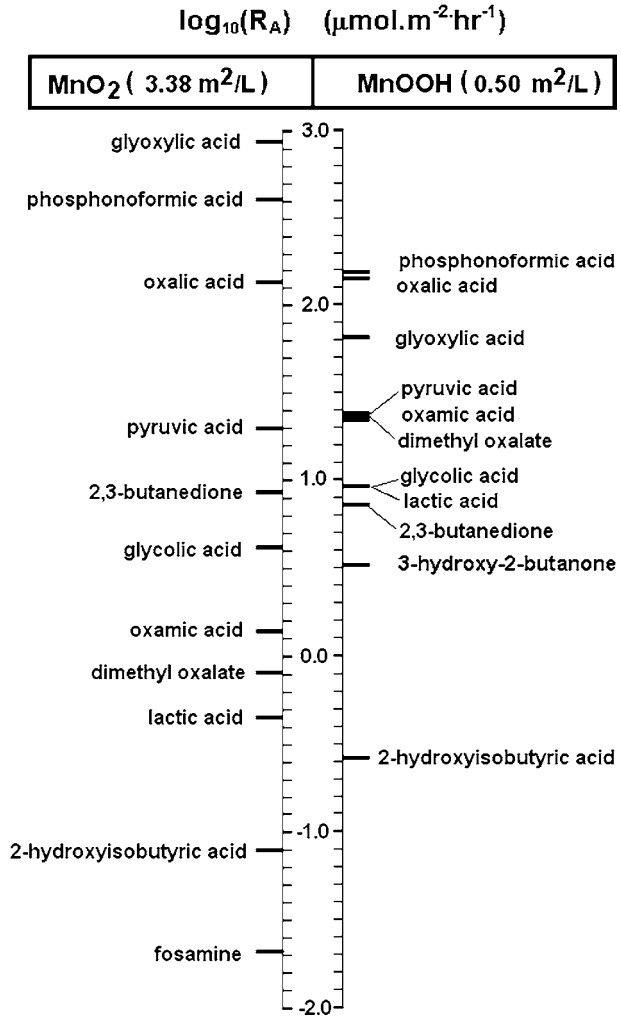

Fig. 9. A comparison of reaction rates with MnO_2 and with MnOOH at pH 5.0. R_A (with units of μmol m^{-2} h^{-1}) corrects for differences in surface area loading for the two (hydr)oxides by dividing R_0 by the surface area (in m^2 g^{-1}), the formula weight (in g/mol Mn), and the suspension concentration (in moles Mn/L). R_0 values were derived from the time course plots presented in Figs. 3 and 4.

The most dramatic differences between the two (hydr)oxides arise with the following organic reactants. Glyoxylic acid reacts 14-times faster with MnO_2 than with MnOOH. MnO_2 reacts more slowly than MnOOH by a factor of 1/16th with oxamic acid, 1/20th with lactic acid, and 1/33rd with dimethyl oxalate.

With both (hydr)oxides, α-carbonyl carboxylic acids react more quickly than α-hydroxycarboxylic acids (i.e., glyoxylic acid > glycolic acid and pyruvic acid > lactic acid). With MnOOH, an α-diketone (2,3-butanedione) reacts 2.3-times more rapidly than the corresponding α-hydroxyketone (3-hydroxy-2-butanone) (Reaction of 3-hydroxy-2-butanone with MnO_2 was not investigated.). With both (hydr)oxides, glyoxylic acid reacts more rapidly than pyruvic acid. Although MnOOH reacts at the same rate with glycolic acid and lactic acid, MnO_2 reacts 8.8-times faster with the former. With both (hydr)oxides, oxalic acid reacts more rapidly than either oxamic acid or dimethyl oxalate. 2-Hydroxyisobutyric acid has the same structure as lactic acid except that the hydrogen on the α-carbon has been replaced by a methyl group. As a consequence, 2-hydroxyisobutyric acid yields a reaction rate with MnO_2 that is 1/6th the rate obtained with lactic acid. For reaction with MnOOH, the rate with 2-hydroxyisobutyric acid is 1/36th the rate with lactic acid.

3.7. Reaction pathways—an overview

Five reaction pathways may take place in our suspensions:

$$\text{(I) Adsorption: } > Mn^{III,IV} + L(aq) \leftrightarrow > Mn^{III,IV}L \quad (3)$$

$$\text{(II) Ligand-assisted dissolution: } > Mn^{III,IV}L \rightarrow Mn^{III}L(aq)(+ > Mn^{III,IV}) \quad (4)$$

$$\text{(III) Reductive dissolution: } > Mn^{III,IV}L \rightarrow Mn^{2+}(aq) + L_{ox}(aq)(+ > Mn^{III,IV}) \quad (5)$$

$$\text{(IV) Intramolecular electron transfer: } Mn\ ^{III}L(aq) \rightarrow Mn^{2+}(aq) + L_{ox}(aq) \quad (6)$$

$$\text{(V) Mn-to-Mn electron transfer: } Mn^{2+}(aq) + L(aq) \leftrightarrow Mn^{II}L(aq) \quad (7)$$

$$> Mn^{III,IV} + Mn^{II}L(aq) \rightarrow Mn^{III}L(aq) + Mn^{2+}(aq)(+ > Mn^{III,IV}) \quad (8)$$

These pathway descriptions ignore proton levels and detailed species descriptions (e.g., 1:1 versus 1:2 complexes in solution). L denotes the organic reactant and L_{ox} denotes its oxidized product(s). $>Mn^{III,IV}$ denotes unoccupied surface sites, $>Mn^{III,IV}L$ denotes the organic reactant–surface site complex, and $Mn^{III}L(aq)$ denotes dissolved Mn^{III} complexes. Detachment of a surface-bound Mn atom may uncover new reactive sites (denoted in parentheses).

When Pathway V is significant, autocatalytic time course behavior is observed, as in our recent study of the

reduction of MnO_2(s) by citric acid (Wang and Stone, 2006). Since autocatalytic time course behavior was not observed with any of the compounds listed in Table 1, this pathway can be ignored.

3.7.1. Ligand-assisted dissolution (Pathways I and II)

Dissolved Mn^{IV} complexes are unusual (Cotton et al., 1999); the compounds in Table 1 do not possess the properties necessary to solubilize this oxidation state. For this reason, any dissolution not accompanied by a change in oxidation state must involve Mn^{III}. Solubility considerations are important, since dissolution cannot proceed if reaction thermodynamics are unfavorable. Consider the following reactions:

$$MnOOH(s) + 3H^+ = Mn^{3+}(aq) + 2\ H_2O \quad {}^*K_{so} \tag{9}$$

$$Mn^{3+} + xH^+ + yL^{n-} = [\ Mn^{III}H_xL_y]^{(3+x-ny)} \quad K_L \tag{10}$$

$$\text{Add: } MnOOH(s) + (3+x)H^+ + y\ L^{n-} = [Mn^{III}H_xL_y]^{(3+x-ny)} + 2H_2O \tag{11}$$

$$K_{Overall} = {}^*K_{so}K_L$$

Hence:

$$[Mn^{III}H_xL_y]^{(3+x-ny)} = {}^*K_{so}K_L][H^+]^{(3+x)}[L^{n-}]^y a_{MnOOH} \tag{12}$$

In the Electronic annex, we derive an estimate of ${}^*K_{so}$, then use complex formation constants for 1:1, 1:2, and 1:3 complexes to estimate the solubility of Mn^{III} in the presence of oxalic acid. According to our calculations (Fig. S1, Electronic annex), 5.0 mM oxalic acid is capable of solubilizing 200 μM MnOOH(s) at pH 5.0. Raising the pH to 6.0, however, lowers solubility to the point that ligand-assisted dissolution cannot be significant.

The possibility of appreciable Mn^{III}(aq) can be dismissed for all the other organic reactants listed in Table 1, except for phosphonoformic acid. Ligands bearing a sole carboxylic acid group (or phosphonate monoester group) are not strong enough to solubilize sparingly-soluble metal ions like Mn^{III}. Aldehyde oxygens, ketone oxygens, and amide nitrogens are exceedingly weak Lewis Bases, and hence contribute little. With glycolic acid, lactic acid, and 2-hydroxyisobutyric acid, high pK_as of the –OH groups (higher than that of ethanol) are a barrier to chelate formation. Complex formation constants with Mn^{III} have not been reported. Complex formation constants for Fe^{III} complexes with glycolic acid and lactic acid available in the literature (Portanova et al., 2003) are significantly lower in magnitude than those for Fe^{III} with oxalic acid. It is probably correct to assume that complexes with Mn^{III} are also weak.

Replacing a carboxylate group with a phosphonate group generally increases log$K$s for complex formation, owing to higher charge and higher basicity (Kiss and Lazar, 2000). The fact that 5.0 mM phosphonoformic acid yields nearly complete conversion of MnOOH(s) to Mn^{III}(aq) at pHs 6.0 and 7.0 lends support to the idea that phosphonoformic acid is a stronger chelating agent for Mn^{III} than oxalic acid.

Recall that 22% of the Mn atoms within our MnO_2(s) preparation are in the +III oxidation state. Redox-inert chelating agents pyrophosphoric acid, methylenediphosphonic acid, and phosphonoacetic acid are capable of solubilizing Mn^{III} from this phase, as well as from MnOOH (Wang, 2005). Our observation in the present work that dissolved Mn^{III} is not seen in the reaction of phosphonoformic acid with MnO_2 indicates that a competing redox reaction is predominant.

3.7.2. Ligand-assisted dissolution followed by intramolecular electron transfer (Pathways I, II, and IV)

Oxalic acid and phosphonoformic acid are reducing agents as well as chelating agents. The following scheme needs to be considered: adsorption followed by ligand-assisted dissolution yields Mn^{III} complexes in solution, which then undergo intramolecular electron transfer, yielding Mn^{II}(aq) and oxidized chelating agent.

As far as reaction with oxalic acid is concerned, we have to account for the fact that appreciable concentrations of dissolved Mn^{III} were not observed. The scheme under consideration will yield this result only if rate constants for the consumption of dissolved Mn^{III} (via intramolecular electron transfer) are higher than rate constants for its production (via ligand-assisted dissolution).

Taube (1948) reported first-order rate constants for breakdown via intramolecular electron transfer for the following species in 2.0 M KCl: $1.97\times10^{-1}\ s^{-1}$ for $Mn^{III}(oxalate)^+$, $7.7\times10^{-4}\ s^{-1}$ for $Mn^{III}(oxalate)_2^-$, and $3.42\times10^{-4}\ s^{-1}$ for $Mn^{III}(oxalate)_3^{3-}$. In the Electronic annex, we have calculated overall Mn^{II} production rates based upon the assumption that all three Mn^{III}-oxalate species are in instantaneous equilibrium with the solid phase. For comparison with the oxalic acid entry in Table 1, we performed this calculation for pH 5.0 in the presence of 5.0 mM oxalic acid. Calculated Mn^{II} production rates exceed actual rates observed with either MnOOH or with MnO_2. For comparison with Fig. 6, we have repeated this calculation using 200 μM oxalic acid (see Fig. S2, Electronic annex). At pH 4.3, the calculated rate is 2.5-times slower than the measured Mn^{II} production rate. This discrepancy increases as the pH is increased. At pH 6.9, the calculated rate is 6800-times slower than the measured rate. The assumption of instantaneous equilibrium among Mn^{III} species yields, of course, the uppermost limit for reaction via this scheme; our own experience indicates that ligand-assisted dissolution reactions are slower than this. Hence, we can conclude that ligand-assisted dissolution followed by intramolecular electron transfer may be a possibility when 5.0 mM oxalic acid is employed, but not when 200 μM oxalic acid is employed.

Dissolved Mn^{III}-phosphonoformate complexes formed by ligand-assisted dissolution of MnOOH(s) at pH 7.0 are stable on timescales of at least 150 h (Fig. 8). Any such complexes formed by ligand-assisted dissolution of MnO_2(s) at pH 7.0 should also be stable. Since dissolved Mn^{III} species

were not observed despite considerable production of dissolved Mn, we can conclude that phosphonoformate reacts with MnO_2(s) at pH 7.0 solely via reductive dissolution.

What about reactions with phosphonoformic acid at lower pH values? Although Mn^{III}-phosphonoformate complexes are still important products of reaction with MnOOH(s), their contribution to total dissolved Mn decreases as the pH is decreased to 6.0 and then to 5.0. Two possibilities exist: (i) ligand-assisted dissolution still predominates, but dissolved Mn^{III}-phosphonoformate complexes break down more rapidly (via intramolecular electron transfer) as the pH is decreased and (ii) Ligand-assisted dissolution and reductive dissolution take place as parallel reactions, with the latter increasing in importance as the pH is decreased. At pHs 6.0 and 5.0, phosphonoformate dissolves MnO_2(s) more rapidly than MnOOH(s). Again, the identity of the Mn (hydr)oxide under investigation should not affect timescales for breakdown of dissolved Mn^{III}-phosphonoformate complexes. Since such complexes were not observed during reaction of phosphonoformate with MnO_2(s), we can conclude that reductive dissolution predominates.

By process of elimination, we have reached the following conclusions regarding dissolution pathways:

Phosphonoformic acid + MnOOH	➢ Pure ligand-assisted dissolution at pH 7.0. ➢ Ligand-assisted dissolution combined with either intramolecular electron transfer or reductive dissolution at pH 5.0 and 6.0.
Phosphonoformic acid + MnO_2	➢ Pure reductive dissolution.
Oxalic acid + MnOOH	➢ Pure reductive dissolution when 200 μM oxalic acid is employed.
Oxalic acid + MnO_2	➢ Reductive dissolution with the possibility of ligand-assisted dissolution/ intramolecular electron transfer when 5.0 mM oxalic acid is employed.
All other organic reactants + MnOOH All other organic reactants + MnO_2	➢ Pure reductive dissolution.

3.7.3. Reductive dissolution (Pathways I and III)

Of the experiments listed in Table 1, only the MnOOH + phosphonoformic acid yielded any dissolved Mn^{III} (for that entry, we report a corrected rate representing Mn^{II} production only). Fig. 6, which shows MnO_2 dissolution as a function of pH in the presence of glyoxylic acid, phosphonoformic acid, and oxalic acid, once again deals solely with Mn^{II} production. Hence, we have a rich data set for discussing the reductive dissolution pathway.

Overall rates of Mn^{II}(aq) production are proportional to the precursor complex formed during the adsorption step. A few points need to be made. Electron transfer may take place via an inner-sphere precursor complex, an outer-sphere precursor complex, or both, depending upon the identity of the reactants and prevalent conditions. The precursor complex may be a minor surface species, i.e., its stoichiometry and bonding arrangements may be different from the predominant form of the adsorbed organic reactant. As two reactions in series, the adsorption step (Pathway I) or the electron transfer step (Pathway III) may be rate-limiting. Regardless of which step is rate-limiting, Mn^{II} production and oxidized organic product (L_{ox}) production are proportional to the precursor complex concentration:

$$\frac{dMn^{II}(aq)}{dt} = w\frac{d[L_{ox}]}{dt} = k_{III}[> Mn^{III,IV}L] \quad (13)$$

where w is a stoichiometric coefficient that accounts for reducing equivalents (per mole of organic reactant oxidized) and oxidizing equivalents (per mole of Mn reduced).

The surface area loading in experiments involving MnO_2 is 6.5-times higher than in experiments involving MnOOH. R_A values account for this difference in surface area loading, but cannot account for chemical differences between the two (hydr)oxide surfaces. MnOOH (manganite) is a non-ion exchanging phase with a pH_{zpc} of 8.1 (Ramstedt et al., 2004), structurally similar to AlOOH (boehmite) and FeOOH (lepidocrocite) (Wells, 1984). Carboxylate adsorption onto Al^{III} (hydr)oxides (Kummert and Stumm, 1980) and phosphonate adsorption onto Fe^{III} (hydr)oxides (Nowack and Stone, 1999) exhibits what is known as "anion-like" adsorption (Stumm, 1992), i.e., increasing adsorption with decreasing pH until a maximum value is reached. We expect that organic reactant adsorption onto MnOOH follows a similar pH dependence. MnO_2 (birnessite) is a layered phase (Post and Veblen, 1990) with strong cation-exchange properties and a pH_{zpc} of 2.3 (Murray, 1974; Tonkin et al., 2004). As discussed in an earlier section, adsorption of methylphosphonic acid and acetic acid onto MnO_2 exhibits a similar pH dependence to what we have proposed for MnOOH. However, an exceptionally high loading is required to yield an appreciable extent of anion adsorption. The low pH_{zpc} of the MnO_2 surface in comparison to more commonly studied (hydr)oxides indicates that it is harder to protonate surface-bound oxygen atoms. O^{2-} and OH^- are poorer exiting ligands than H_2O, hence it is energetically more difficult for organic reactant molecules to enter the inner coordination sphere. Per unit area loading, our expectation is that MnO_2 is substantially poorer at adsorbing organic reactants than MnOOH.

Comparisons of R_A values between the two (hydr)oxides must be made with caution. A low extent of adsorption may

be compensated for by a high rate of electron transfer within the adsorbed species, and vice versa. Our inability to resolve changes in extents of adsorption from changes in rates of electron transfer within the surface precursor complex most notably affects our ability to explain differences in pH dependence among different organic reactants (i.e., glyoxylic acid, phosphonoformic acid, and oxalic acid in Fig. 6).

In MnOOH suspensions, Mn^{III} is the sole oxidant. The fact that MnO_2, consisting of 22% Mn^{III} and 78% Mn^{IV}, reacts faster than MnOOH with some organic reactants yet slower with others is intriguing. Does this mean that some reactants react more rapidly with Mn^{IV}, while others react more rapidly with Mn^{III}? Are we seeing the effects of (hydr)oxide structure or differences in protonation/deprotonation behavior, as reflected in their corresponding pH_{zpc} values? Results from a (hydr)oxide phase consisting solely of Mn^{IV}, or with a pure Mn^{III} with markedly different structural features (e.g., MnOOH(feitknecktite)) would provide valuable comparisons.

The lists of organic compounds known to reduce $Mn^{III,IV}$ (hydr)oxides has now been expanded to include neutral compounds such as dimethyl oxalate, 2,3-butanedione, and 3-hydroxy-2-butanone. Phosphonoformic acid, similar to oxalic acid in many ways yet distinctive in others, provides a unique opportunity to study ligand-assisted dissolution and reductive dissolution reactions in competition with one another. It is noteworthy that glyoxylic acid is more reactive than oxalic acid when the oxidant is MnO_2, yet less reactive than oxalic acid when the oxidant is MnOOH. Reactant-to-reactant comparisons may one day allow us to distinguish the reactivity of surface-bound Mn^{III} from surface-bound Mn^{IV}.

Acknowledgments

This work was supported by Grant No. R-82935601 from the U.S. Environmental Protection Agency's Science to Achieve Results (STAR) program. Although the research described in this article has been funded wholly by this Grant, it has not been subject to EPA review and therefore does not necessarily reflect the views of the Agency, and no official endorsement should be inferred. We thank Dr. Anne-Claire Gaillot (Department of Earth and Planetary Sciences, Johns Hopkins University) for her help with MnO_2 (birnessite) and MnOOH (manganite) characterization, Prof. James J. Morgan, and two anonymous reviewers for thoughtful discussion and insightful comments.

Associate editor: George R. Helz

Appendix A. Supplementary data

Supplementary data associated with this article can be found, in the online version, at doi:10.1016/j.gca.2006.06.1548.

References

Afif, E., Barron, V., Torrent, J., 1995. Organic-matter delays but does not prevent phosphate sorption by Cerrado soils from Brazil. *Soil Sci.* **159**, 207–211.

Bricker, O., 1965. Some stability relations in system $Mn–O_2–H_2O$ at 25 degrees and 1 atmosphere total pressure. *Am. Mineral.* **50**, 1296–1354.

Cotton, F.A., Wilkinson, G., Murillo, C.A., Bochmann, M., 1999. *Advanced Inorganic Chemistry*. Wiley Interscience, New York.

Drummond, A.Y., Waters, W.A., 1955. Stages in oxidations of organic compounds by potassium permanganate. 6. Oxidations of ketones and of pyruvic acid. *J. Chem. Soc.*, 497–504.

Filius, J.D., Hiemstra, T., Van Riemsdijk, W.H., 1997. Adsorption of small weak organic acids on goethite: modeling of mechanisms. *J. Colloid Interf. Sci.* **195**, 368–380.

Fox, T.R., Comerford, N.B., 1990. Low-molecular-weight organic-acids in selected forest soils of the southeastern USA. *Soil Sci. Soc. Am. J.* **54**, 1139–1144.

Furrer, G., Stumm, W., 1986. The coordination chemistry of weathering. 1. Dissolution kinetics of δ-Al_2O_3 and BeO. *Geochim. Cosmochim. Acta* **50**, 1847–1860.

Giovanoli, R., Leuenberger, U., 1969. Oxidation of manganese oxide hydroxide. *Helv. Chim. Acta* **52**, 2333–2347.

Godtfredsen, K.L., Stone, A.T., 1994. Solubilization of manganese dioxide-bound copper by naturally occurring organic compounds. *Environ. Sci. Technol.* **28**, 1450–1458.

Guest, C.A., Schulze, D.G., Thompson, I.A., Huber, D.M., 2002. Correlating manganese X-ray absorption near-edge structure spectra with extractable soil manganese. *Soil Sci. Soc. Am. J.* **66**, 1172–1181.

Haight, G.P., Jursich, G.M., Kelso, M.T., Merrill, P.J., 1985. Kinetics and mechanisms of oxidation of lactic-acid by chromium(VI) and chromium(V). *Inorg. Chem.* **24**, 2740–2746.

Hasan, F., Rocek, J., 1975. 3-Electron oxidations. 9. Chromic acid oxidation of glycolic acid. *J. Am. Chem. Soc.* **97**, 1444–1450.

Jauregui, M.A., Reisenauer, H.M., 1982. Dissolution of oxides of manganese and iron by root exudate components. *Soil Sci. Soc. Am. J.* **46**, 314–317.

Kalhorn, S., Emerson, S., 1984. The oxidation-state of manganese in surface sediments of the deep-sea. *Geochim. Cosmochim. Acta* **48**, 897–902.

Kemp, T.J., Waters, W.A., 1964. Kinetic study of oxidations of formaldehyde + formic acid by manganic sulphate. *J. Chem. Soc. (JAN)*, 339–347.

Kiss, T., Lazar, I., 2000. Structure and stability of metal complexes in solution. In: Kukhar, V.P., Hudson, H.R. (Eds.), *Aminophosphonic and Aminophosphinic Acids*. Wiley, New York, pp. 284–323.

Klewicki, J.K., Morgan, J.J., 1999. Dissolution of β-MnOOH particles by ligands: pyrophosphate, ethylenediaminetetraacetate, and citrate. *Geochim. Cosmochim. Acta* **63**, 3017–3024.

Kostka, J.E., Luther, G.W., Nealson, K.H., 1995. Chemical and biological reduction of Mn(III)-pyrophosphate complexes—potential importance of dissolved Mn(III) as an environmental oxidant. *Geochim. Cosmochim. Acta* **59**, 885–894.

Krumpolc, M., Rocek, J., 1977. 3-Electron oxidations. 12. Chromium(V) formation in chromic-acid oxidation of 2-hydroxy-2-methylbutyric acid. *J. Am. Chem. Soc.* **99**, 137–143.

Krumpolc, M., Rocek, J., 1985. Chromium(V) oxidations of organic-compounds. *Inorg. Chem.* **24**, 617–621.

Kummert, R., Stumm, W., 1980. The surface complexation of organic-acids on hydrous γ-Al_2O_3. *J. Colloid Interf. Sci.* **75**, 373–385.

Leitner, N.K.V., Berger, P., Legube, B., 2002. Oxidation of amino groups by hydroxyl radicals in relation to the oxidation degree of the α-carbon. *Environ. Sci. Technol.* **36**, 3083–3089.

Levesley, P., Waters, W.A., 1955. Stages in oxidations of organic compounds by potassium permanganate. 5. Oxidations of some

alpha-hydroxy-acids by manganic pyrophosphate. *J. Chem. Soc.*, 217–221.

Lindqvist, C., Nordstrom, T., 2001. Generation of hydroxyl radicals by the antiviral compound phosphonoformic acid (forscarnet). *Pharmacol. Toxicol.* **89**, 49–55.

Luo, J.A., Zhang, Q.H., Suib, S.L., 2000. Mechanistic and kinetic studies of crystallization of birnessite. *Inorg. Chem.* **39**, 741–747.

Luther, G.W., Ruppel, D.T., Burkhard, C.A., 1999. Reactivity of dissolved Mn(III) complexes and Mn(IV) species with reductants: Mn redox chemistry without a dissolution step? In: Sparks, D.L., Grundl, T.J. (Eds.), *Mineral–Water Interfacial Reactions: Kinetics and Mechanisms*. American Chemical Society, Washington, DC, pp. 265–280.

Madigan, M.T., Martinko, J.M., Parker, J., 2002. *Brock Biology of Microorganisms*. Prentice Hall, Upper Saddle River, NJ.

Marschner, H., 1995. *Mineral Nutrition of Higher Plants*. Academic Press, New York.

Martell, A.E., Smith, R.M., Motekaitis, R.J., 2004. NIST Critically Selected Stability Constants of Metal Complexes Database. US Department of Commerce, National Institute of Standards and Technology.

Murray, J.W., 1974. Surface chemistry of hydrous manganese-dioxide. *J. Colloid Interf. Sci.* **46**, 357–371.

Murray, J.W., Balistrieri, L.S., Paul, B., 1984. The oxidation-state of manganese in marine-sediments and ferromanganese nodules. *Geochim. Cosmochim. Acta* **48**, 1237–1247.

Nowack, B., Stone, A.T., 1999. Adsorption of phosphonates onto the goethite–water interface. *J. Colloid Interf. Sci.* **214**, 20–30.

Portanova, R., Lajunen, L.H.J., Tolazzi, M., Piispanen, J., 2003. Critical evaluation of stability constants for α-hydroxycarboxylic acid complexes with protons and metal ions and the accompanying enthalpy changes Part II. Aliphatic 2-hydroxycarboxylic acids. *Pure Appl. Chem.* **75**, 495–540.

Post, J.E., Veblen, D.R., 1990. Crystal-structure determinations of synthetic sodium, magnesium, and potassium birnessite using TEM and the Rietveld method. *Am. Mineral.* **75**, 477–489.

Ramstedt, M., Andersson, B.M., Shchukarev, A., Sjoberg, S., 2004. Surface properties of hydrous manganite (γ-MnOOH). A potentiometric, electroacoustic, and X-ray photoelectron spectroscopy study. *Langmuir* **20**, 8224–8229.

Schecher, W.D., McAvoy, D.C., 2003. MINEQL+: A Chemical Equilibrium Modeling System, Version 4.5 for Windows, User's Manual, Environmental Research Software, Hallowell, ME.

Sellers, R.M., 1983. The radiation-chemistry of nuclear-reactor decontaminating reagents. *Radiat. Phys. Chem.* **21**, 295–305.

Stone, A.T., 1987a. Microbial metabolites and the reductive dissolution of manganese oxides–oxalate and pyruvate. *Geochim. Cosmochim. Acta* **51**, 919–925.

Stone, A.T., 1987b. Reductive dissolution of manganese(III/IV) oxides by substituted phenols. *Environ. Sci. Technol.* **21**, 979–988.

Stone, A.T., 1997. Reaction of extracellular organic ligands with dissolved metal ions and mineral surfaces. In: Banfield, J., Nealson, K. (Eds.), *Geomicrobiology: Interactions between Microbes and Minerals*. Mineralogical Society of America, Washington, DC, pp. 309–344.

Stone, A.T., Godtfredsen, K.L., Deng, B.L., 1994. Sources and reactivity of reductants encountered in aquatic environments. In: Bidoglio, G., Stumm, W. (Eds.), *Chemistry of Aquatic Systems: Local and Global Perspectives*. Kluwer, Dordrecht, The Netherlands, pp. 337–374.

Stumm, W., 1992. *Chemistry of the Solid–Water Interface: Processes at the Mineral–Water and Particle–Water Interface in Natural Systems*. John Wiley, New York.

Stumm, W., Morgan, J.J., 1996. *Aquatic Chemistry—Chemical Equilibria and Rates in Natural Waters*. John Wiley, New York.

Taube, H., 1948. The interaction of manganic ion and oxalate—rates, equilibria and mechanism. *J. Am. Chem. Soc.* **70**, 1216–1220.

Thomas, J.K., Trudel, G., Bywater, S., 1960. The reaction of ferric ion with acetoin (3-hydroxy-2-butanone) in aqueous solution. *J. Phys. Chem.* **64**, 51–54.

Tonkin, J.W., Balistrieri, L.S., Murray, J.W., 2004. Modeling sorption of divalent metal cations on hydrous manganese oxide using the diffuse double layer model. *Appl. Geochem.* **19**, 29–53.

Wang, Y., 2005. Electron transfer and coordination reactions between $Mn^{III,IV}O_2$(birnessite, $Mn^{III}OOH$(manganite), and oxygen-donor aliphatic compounds. Ph.D. Thesis, The Johns Hopkins University, Baltimore, MD.

Wang, Y., Stone, A.T., 2006. The citric acid-$Mn^{III,IV}O_2$(birnessite) reaction. Electron transfer, complex formation, and autocatalytic feedback. *Geochim. Cosmochim. Acta*. **70**, 4463–4476.

Ware, G.W., 2000. *The Pesticide Book*. Thomson Publ., Fresno, CA.

Wells, A.F., 1984. *Structural Inorganic Chemistry*. Clarendon Press, Oxford, UK.

Woodburn, K.B., Fontaine, D.D., Bjerke, E.L., Kallos, G.J., 1989. Photolysis of picloram in dilute aqueous-solution. *Environ. Toxicol. Chem.* **8**, 769–775.

Xyla, A.G., Sulzberger, B., Luther, G.W., Hering, J.G., Vancappellen, P., Stumm, W., 1992. Reductive dissolution of manganese(III,IV) (hydr)oxides by oxalate—the effect of pH and light. *Langmuir* **8**, 95–103.